Algerian Journal of Materials Chemistry

Alg. J Mat Chem ISSN 2661-7196 Vol.2 Issue 2, pp 86–100, (2019)

# Preparation, characterization and properties of antimicrobial nanocomposites based on chitosan and modified bentonite

**Soumia Abdelkrim[1], Adel Mokhtar[1, 2*], Abdelkader Bengueddach[1] & Mohamed Sassi[1]**

[1]Laboratoire de Chimie des Matériaux (LCM), Faculté des Sciences Exactes et Appliquées, Université Oran1, BP 1524, Oran El M'Naouer, 31000 Oran, Algeria.
[2]Département Génie des Procédés, Institut des Sciences et Technologies, Centre Universitaire Ahmed Zabana Relizane, Algeria

Received: 08 September 2019 /Accepted: 22 October 2019 /Published online: 29 October 2019

**Abstract**. In the present work, Chitosan/bentonite, Chitosan/Ag-Bentonite and Chitosan/AgNPs-Bentonite composite materials were prepared and shaped in form of beads, and characterized using several methods. After that, their thermal stability, swelling properties and antibacterial and antifungal activity were evaluated. In the case of Chitosan/AgNPs-Bentonite, the XRD analysis confirms the partial intercalation of chitosan in the interlayer of bentonite and the formation of silver nanoparticles, AgNPs, with an average diameter between 10nm and 25nm. The latter is confirmed by UV-Visible diffuse reflectance (UV-Vis DR) spectroscopy by the apparition of the large absorption band at 442 nm. For all prepared materials, the FTIR analysis shows the presence of strong interaction between chitosan reactive groups and bentonite interlayer materials. This result is confirmed by thermal analysis where it is observed that these composite materials exhibit a higher thermal stability than the biopolymer alone. The composite materials present also a very good swelling capacity. Indeed, the swelling rate carried out in water media at pH 7 and a temperature of 30°C is 160% higher than that of the corresponding dried material. Otherwise, Chitosan/AgNPs-Bentonite sample displays a very high antibacterial activity against pathogen bacteria strains such as Staphylococcus aureus ATCC 25923 and Pseudomonas aeruginosa ATCC 27853. This activity is less important for Staphylococcus aureus ATCC 43300 and no activity is observed for Escherichia coli ATCC 25922 and Candida albicans ATCC 10231. Since the starting chitosan and bentonite materials showed no antibacterial or antifungal activity, the antibacterial activity of Chitosan/AgNPs-Bentonite sample is attributed to loaded AgNPs species.
**Keywords**: Chitosan; Bentonite; Silver Nanoparticles; Chemical reduction; Swelling; Antimicrobial Activities.

## 1 Introduction

Due to the increasingly pronounced occurrence of conventional antibiotic-resistant bacteria, considerable efforts have been made over the past decade to develop new classes of materials with antibacterial and antifungal activity that can address this public health problem. The basic idea is to use properties of certain metals such as intrinsic antibacterial [1-4], especially silver

* Corresponding author. Adel Mokhtar
-mail address: mokhtar.adel80@yahoo.com ; adel.mokhtar@cu-relizane.dz

nanoparticles. Indeed, the latter are widely applied as an antibacterial agent thanks to the numerous advantages compared to the conventional antimicrobial [5-10], such as chemical stability, safety for the user, a prolonged period and excellent antibacterial activity [11]. However, used alone, silver nanoparticles have disadvantages related to leaching and aggregation phenomena that can generate environmental problems and limit their antibacterial activity. To avoid these limitations and maintain their antibacterial activity for a prolonged time as possible, these nanoparticles can be loaded into solid matrix. This approach will certainly give rise to a new class of environmentally friendly antibacterial materials that retain the antibacterial properties of silver and can be used in many applications. Thus, the recent emergence of new metal matrix-supported antibacterial materials has been a very promising alternative to conventional antimicrobials [12, 13]. Indeed, these materials have found several applications in the coating for manufacturing medical instruments [14], in agriculture [15, 16].
Clay minerals are a good support of metals ions [17, 18]. The low cost and eco-friendly are most important upsides of these solids [19]. Their high specific surface area and cation exchange capacity, and their good thermal and chemical stability provide them a various of surface and structural properties. This makes them excellent support for metallic nanoparticles [20, 21], a good adsorption [22, 23] and high dispersion. Due to their 2:1 arrangement [24], bentonite is able to expand and contract the interlayer space while preserving two-dimensional crystallographic integrity. In this context, researchers have recently multiplied efforts by combining the characteristics of this material with those of other inorganic or organic substances in order to obtain novel hybrid materials with singular properties that have achieved interesting results in the fields of the environment [25, 26] and biology [27, 28].

Chitosan, the deacetylated product of chitin, is the second-most abundant biopolymer in nature [29]. This anionic polysaccharide has several intrinsic characteristics that make it an effective biosorbent for the removal of many pollutants and is also used in medical applications [30, 31]. Its use as a biosorbent is justified by numerous advantages and properties such as low cost compared to others materials, biodegradability, environmentally friendly, non-toxicity and abundance. Another important property that it can be easily shaped in different forms. However, because to its limited applications due to its moisture permeability and high brittleness [32], it is possible to combine this biopolymer with bentonite to improve its thermal, chemical and mechanical properties.

To our knowledge, no literature review reports the use of natural Algerian bentonite as an antibacterial and antifungal material or in the preparation of biocomposite materials by reaction with a biopolymer, chitosan. Thus, the present work reports the preparation of new AgNPs-nanocomposite materials from Ag-Bentonite and chitosan. All the obtained materials are characterized by X-ray diffraction analysis (XRD), Fourier transforms infrared (FTIR) and UV-Visible diffuse reflectance (UV-Vis DR) spectroscopy and thermal (TG) analysis. The objective is to evaluate the swelling, thermal, antibacterial and antifungal properties. The antibacterial and antifungal properties are evaluated through growth inhibition towards pathogen bacteria strains

such as Staphylococcus aureus ATCC 25923, Escherichia coli ATCC 25922, Staphylococcus aureus ATCC 43300, Pseudomonas aeruginosa ATCC 27853 and Candida albicans ATCC 10231.

## 2 Experimental

### *2.1 Materials*

The natural clay (Bentonite) obtained by deposit of Maghnia west of Algeria [33], silver nitrate ($AgNO_3$; Sigma-Aldrich 99.8-100.5%)**,** **s**odium tetrahydridoborate ($NaBH_4$; Sigma-Aldrich 99%), Sodium Hydroxide (NaOH; Sigma-Aldrich >98%) and biopolymer Chitosan (degree of acetylation of 10% as measured by IR spectroscopy, MW = 700,000 g mol-1 determined by viscosimetry) from crab shell provided from Sigma-Aldrich. Deionized water was used for all preparations.

### *2.2 Preparation of Ag-Bentonite material*

The preparation of Ag-Bentonite sample was carried out by ion-exchange method as follow: 2 g of Bentonite was suspended in deionized water and stirred for 30 min. Then, a silver nitrate solution, prepared by dissolving the required amount of $AgNO_3$ in desionized, water was added. The reaction mixture obtained was vigorously stirred for 24 hours at a temperature of 60°C. The resulting exchanged Ag-Bentonite sample was recovered by filtration, and then dried at a temperature of 80°C for 24 hours.

### *2.3 Preparation of Chitosan/Ag-Bentonite and Chitosan/AgNPs-Bentonite composites beads*

The Chitosan/Ag-Bentonite composite beads is prepared as follow: A solution A is prepared by dispersing 1.5 g of Ag-Bentonite sample in 50 ml of deionized water and stirred for 30 minutes at room temperature. Otherwise, a second solution of chitosan (100 ml, 1wt%) (solution B) is prepared by solubilization of chitosan in acetic acid solution of pH 4.5 under constant stirring for 45 min at 40°C and then filtered to remove the insoluble biopolymer. The two solutions are mixed in a chitosan/Ag-bentonite ratio of 2 and stirred vigorously for two hours at room temperature. The final mixture was then extruded in the form of droplets, using a syringe ~2 mm of diameter, into NaOH solution. The resulting composite beads formed are allowed to stand for one hour in the NaOH solution in order to crosslink. After that, they are filtered and washed several times with distilled water to remove excess of NaOH from the surface. In order to keep their spherical morphology, the beads are immersed in a concentrated ethanol solution to oust water from them and then dried for 24 hours at room temperature.

The preparation procedure of Chitosan/AgNPs-Bentonite is the following: the dried Chitosan/Ag-Bentonite composites beads were immersed for 24 hours into a $NaBH_4$ solution.

After that, they were filtered and washed several times with deionized water to remove un-reacted $NaBH_4$ on the surface of beads and then dried for 24 hours at room temperature.

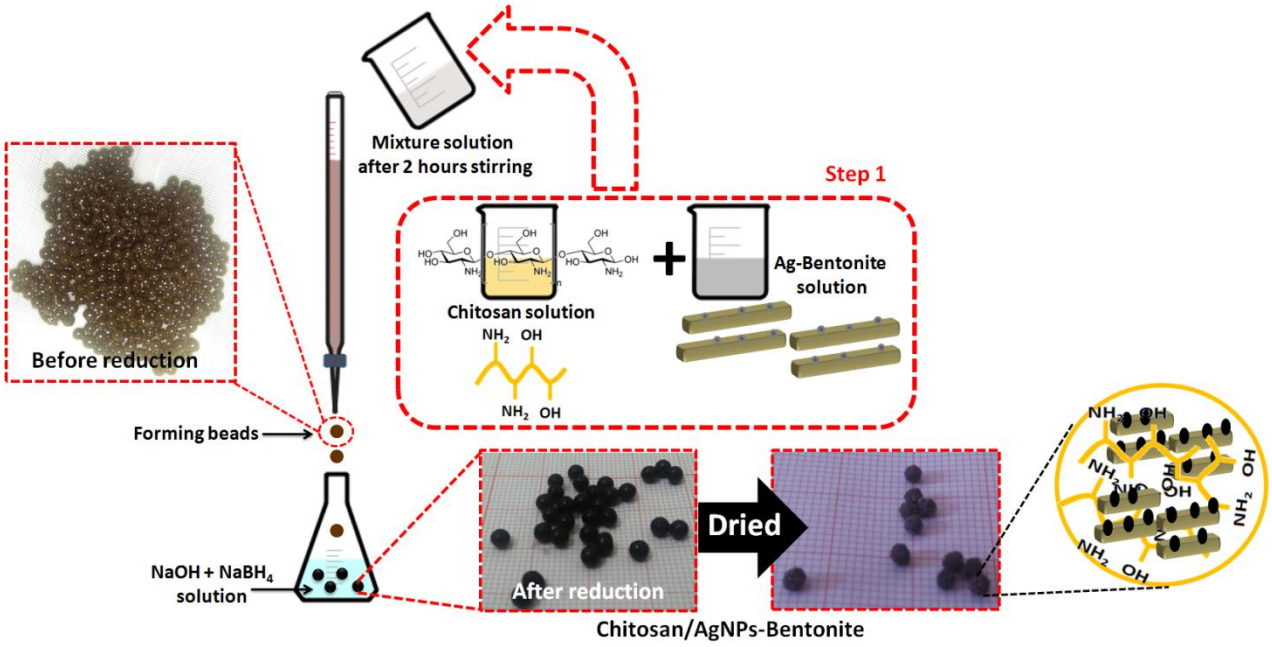


**Fig. 1** Preparation method of Chitosan/AgNPs-Bentonite composite materials with photographed images of corresponding composites beads after 5 days of reaction.

*2.4 Swelling experiment*

The swelling rate of Chitosan/Bentonite, Chitosan/Ag-Bentonite and Chitosan/AgNPs-Bentonite composites materials was determined by immersing the corresponding dried beads in water at pH7 and a temperature of 30°C. The study was carried out until the swelling equilibrium was reached after 500 minutes of immersion, then the composite beads were removed at regular time intervals and weighed after carefully blotting with tissue paper to remove surface water. The swelling rate (%) for each sample was calculated using the following Equation [34, 35]:

$$\text{Swelling rate (\%)} = \frac{W_t - W_0}{W_0} \times 100$$

Where $W_0$ is the initial weight and $W_t$ the final weight of the prepared beads at time t.

*2.5 Preparation of bacterial cultures*

The same method presented in our previous works was used to prepare the bacterial medium [36]. The Chitosan/AgNPs-Bentonite composite beads were tested as antibacterial and antifungal agents against pathogenic bacteria and fungal strains using the dishes inhibition method. A same amount of beads are deposited on the surface of solid mass medium seeded with pure bacterial culture. Pathogenic bacteria strains studied are Staphylococcus aureus ATCC 25923, Escherichia coli ATCC 25922, Staphylococcus aureus ATCC 43300 and Pseudomonas aeruginosa ATCC

27853. For antifungal activity study, Candida albicans ATCC 10231 was used. 0.5 ml culture ($10^8$ cell/ml) obtained after incubation at 37°C for 24 hours was mixed with 10 ml of medium (PDA) liquid at 40°C. The latter, probably solid, is melted by heating and then cooled before placing in contact with the microbial suspension. The mixture was placed in Petri dishes of 90 mm. The Chitosan/AgNPs-Bentonite composite beads, previously sterilized at 180°C for 30 minutes, are then deposited in the bacterial medium carrying the bacteria. The antimicrobial activity is determined after incubation of the dishes in an oven at 37°C for 24 h for bacteria and 48 h at 30°C for Candida albicans. The inhibition zone for bacterial growth was detected visually and immediately photographed.

*2.6 Characterization*

X-ray powder diffraction (XRD) patterns were recorded in the 2θ range of 2-80° at a scan rate 2°/min, on a Philips diffractometer model PW 1830, with Ni-filtered CuKα (λ= 1.5406 Å) radiation operated at a tube voltage of 40 kV and a tube current of 30 mA. The Fourier Transform Infrared (FTIR) spectra were recorded between 400 and 4000 $cm^{-1}$ on a JASCO 4100 spectrometer. Ultraviolet visible (UV–Vis) absorbance spectra were recorded on a Specord 210 Analytik Jena spectrometer with a holmium oxide filter. Thermogravimetric analysis (TGA) was performed on LABSYS Evo SETARAM under nitrogen atmosphere in the temperature range 20-800°C with a heating rate of 10 °C/min.

## 3 Results and discussion

*3.1 X-ray diffraction (XRD) analysis*

XRD patterns of Bentonite, Chitosan, Chitosan/Bentonite, Chitosan/Ag-Bentonite and Chitosan/AgNPs-Bentonite samples are exhibited in **Fig. 2**. The X-ray diffraction pattern of bentonite material exhibits several reflections (00l) corresponding to a basal spacing, d001, of 12.60Å characteristics of the sodic form of such a material. Otherwise, the X-ray diffraction pattern of chitosan shows the presence of all diffractions peaks of this material namely, its two important characteristic crystalline peaks observed at 0.86 nm (10.17° 2θ) and 0.44 nm (20.15° 2θ) and the broad peak belonging to amorphous located at 26.5° 2θ. As shown in the **Fig. 2,** , the dispersion of Ag-Bentonite material in the chitosan matrix leads practically to no change in the basal spacing of the clay mineral suggesting that this biopolymer is not intercalated in the interlayer space of the corresponding Chitosan/Ag-Bentonite sample. For Chitosan/AgNPs-Bentonite sample, the XRD pattern shows a shift of the basal spacing, $d_{001}$, from 12.60Å to 14.74Å indicating probably a partial intercalation of chitosan after reduction of interlayer $Ag^+$ ions into AgNPs species whose characteristic peaks are also present in this pattern at 2θ= 38.42°, 44.47°, 64.74° and 77.61° (JCPDS Number 04-783) [37-39]. The calculated average diameter of these loaded AgNPs species varies between 10nm and 25nm.

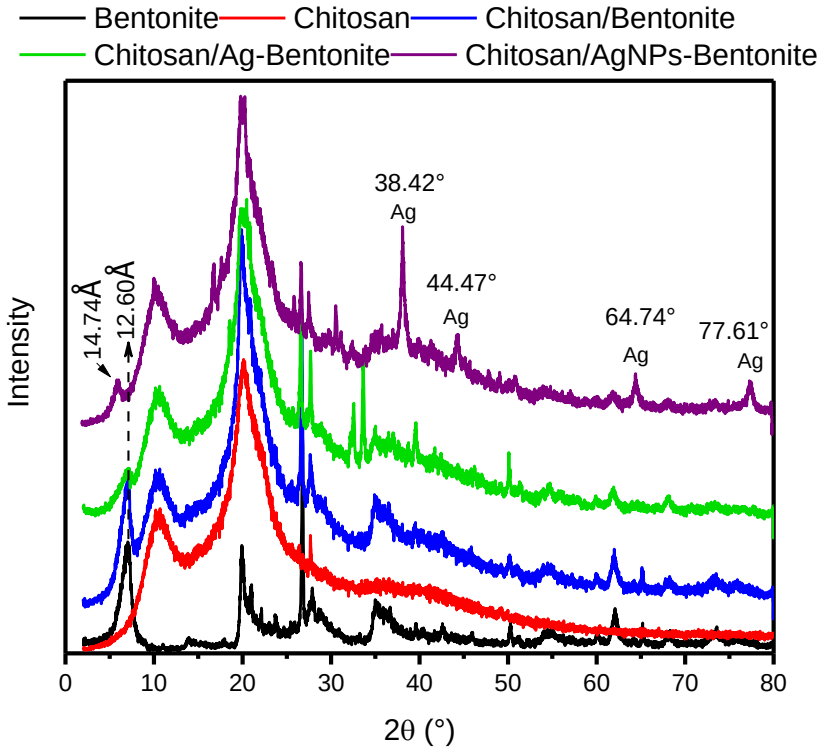


**Fig. 2** X-ray diffraction patterns of Chitosan, Chitosan/Bentonite, Chitosan/Ag-Bentonite and Chitosan/AgNPs-Bentonite materials.

### *3.2 Fourier transforms infrared (FTIR) spectroscopy*

FTIR spectra of Bentonite, Chitosan, Chitosan/Bentonite, Chitosan/Ag-Bentonite and Chitosan/AgNPs-Bentonite samples are displayed in Figure 3. The composite beads spectra show clearly the presence of vibration bands characteristic of the bentonite clay and biopolymer chitosan. The vibration bands of bentonite are observed as follow: the OH stretching band in the region of 3631-3444cm$^{-1}$, the Si─O─Si stretching band in the 1091-1039 cm$^{-1}$ region, and the Si─O stretching vibration band at 795 cm$^{-1}$ [40-42]. The most frequent characteristic absorption bands of the biopolymer assigned to the stretching vibrations of ─CH in ─$CH_2$ and ─$CH_3$ groups appear at 2888 and 2942 cm$^{-1}$, respectively [43]. Those observed at 1590 and 1653 cm$^{-1}$ are assigned to C=O stretching (amide I) and N─H bending (amide II), consecutively [44, 45], and the large absorption band in the region of 3000-3500 cm$^{-1}$ corresponds to O─H stretching, overlapped with N─H stretching [27, 43]. The FTIR analysis gives valuable information concerning the interaction between the mineral material and the biopolymer. Indeed, the vibration band of the interlayer ≡Si-O- groups of bentonite as well as those of ─CH in ─$CH_2$ and ─$CH_3$ groups at 2888 cm$^{-1}$and 2942 cm$^{-1}$, respectively, shifted to the high frequencies for Chitosan/AgNPs-Bentonite material. This shift is due probably to strong interactions between chitosan reactive groups and the mineral matrix, in good agreement with XRD results.

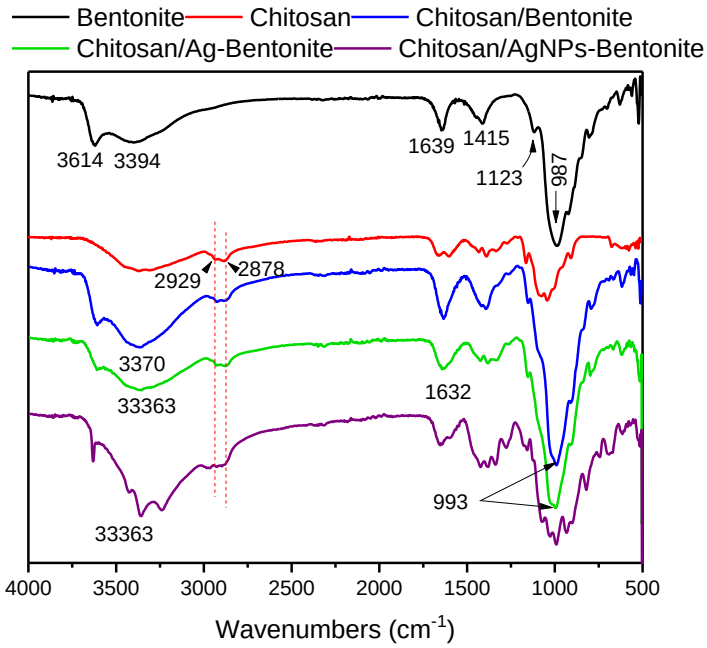


**Fig. 3** FTIR spectra of bentonite, chitosan, Chitosan/Bentonite, Chitosan/Ag-Bentonite and Chitosan/AgNPs-Bentonite materials.

*3.3 UV-Visible diffuse reflectance (UV-Vis DR) spectroscopy analysis*

UV-visible spectroscopy is one of the most generally used techniques for structural characterization of metals species [6, 46]. The UV-vis (DRUV) spectra of samples were presented in **Fig. 4**.

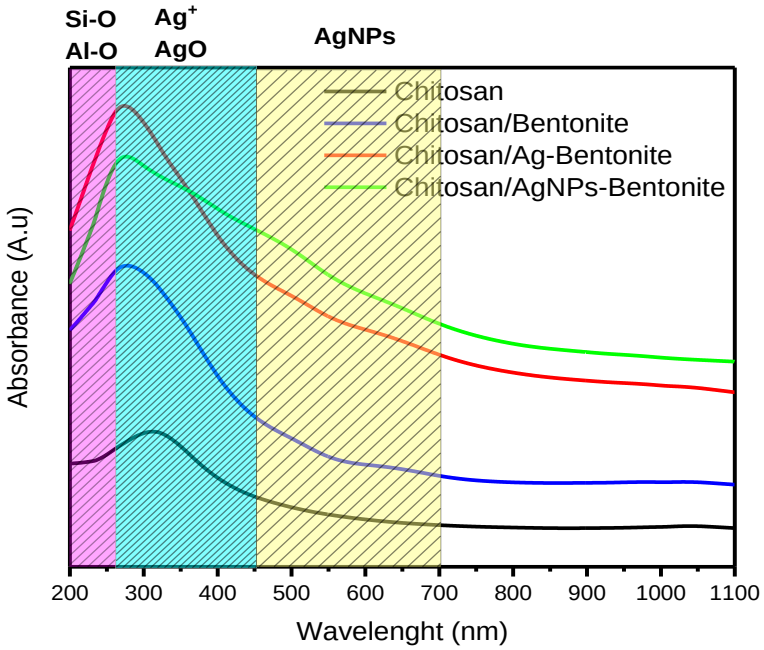

**Fig. 4** UV-vis DR spectra of Chitosan, Chitosan/Bentonite, Chitosan/Ag-Bentonite and Chitosan/AgNPs-Bentonite materials.

All samples showed two absorption bands at 215 nm and 230 nm arising from the Si─O and the Al─O charge-transfer of four coordinated framework silicon and aluminum atoms [36, 47]. Compared to starting bentonite sample each modification in clay mineral either by exchange reaction with silver ions or reduction of this metal by $NaBH_4$ shows a change in adsorption bands. The UV-vis (DRUV) spectrum of Chitosan/AgNPs-Bentonite sample revealed a remarkable broad absorption band in the visible region between 400-650nm attributed to silver nanoparticles, AgNPs, species, [48, 49].

### *3.4 Thermogravimetric (TG) analysis*

TG curves of Bentonite, Chitosan, Chitosan/Bentonite, Chitosan/Ag-Bentonite and Chitosan/AgNPs-Bentonite samples are shown in **Fig. 5.** It can be seen clearly that TG curves of composites beads are practically similar to that of pure chitosan [50]. However, these composites beads present higher decomposition temperatures than that of the biopolymer alone. Otherwise these composite materials have better thermal stability which increases with increasing the clay content of the sample. This result can be explained by the establishment of strong interactions between the reactive groups of chitosan and bentonite interlayer materials such as $Ag^+$, $H^+$ and $Na^+$ cations and terminal interlayer $\equiv Si{-}O^-$ groups, which has the consequence of displacing the decomposition of these materials to high temperatures and thus increase their thermal stability [51, 52].

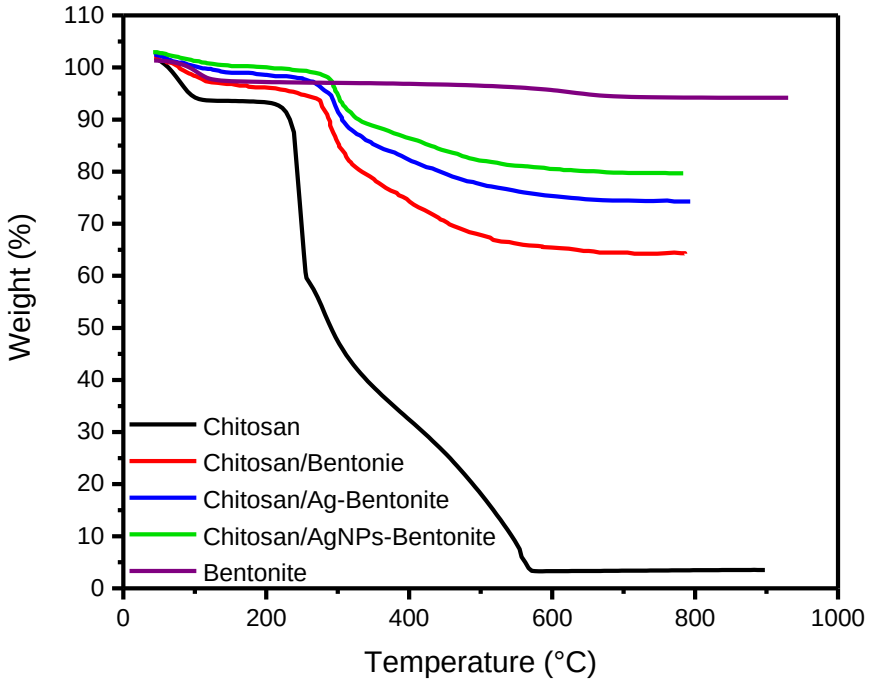


**Fig. 5** TG curves under nitrogen atmosphere for Chitosan, Chitosan/Bentonite, Chitosan/Ag-Bentonite and Chitosan/AgNPs-Bentonite materials.

*3.4 Swelling behavior*

The swelling behavior of the prepared composites beads in the pH 7 at 30°C is presented in **Fig. 5.** Figure 5(b) shows photographed images of composites beads in dried and swelling states. As shown in Fig. 5(a), the swelling increases with time, first quickly then slowly, to reach a plateau after 500 minutes of reaction. Compared to chitosan alone [53, 54], all composite materials exhibit a very high swelling rate which is certainly due to the presence of bentonite. However, the swelling rate of the Chitosan/AgNPs-Bentonite beads was a little lower. This is probably due to the presence of silver species in the interlayer space of Bentonite which leads to an increase in the interaction between the clay and the biopolymer, and consequently a decrease in the swelling rate [55].

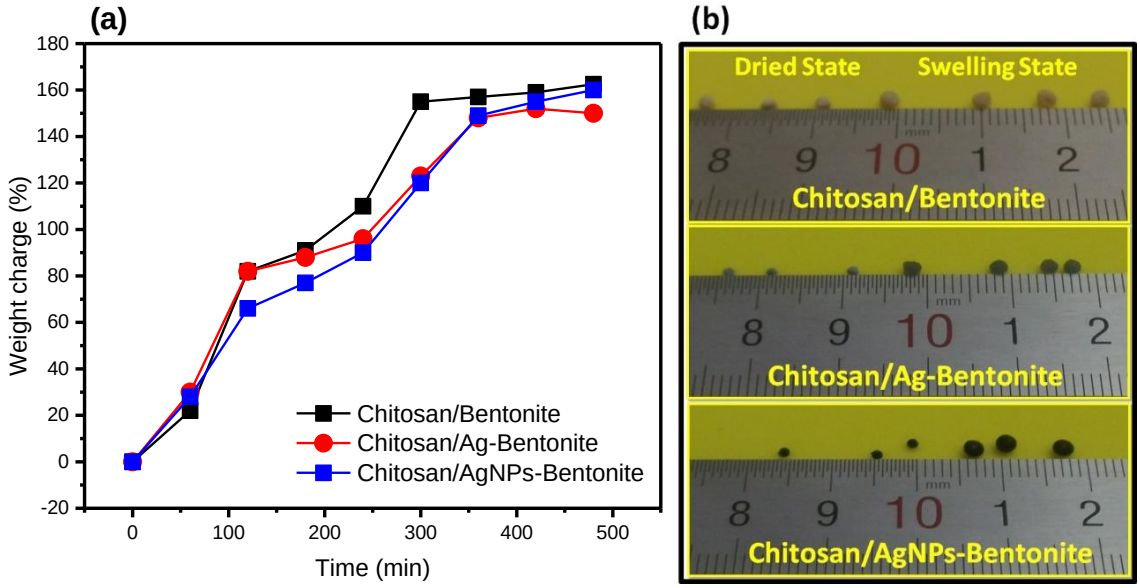


**Fig. 5.** (a) Swelling behavior of Chitosan/Bentonite, Chitosan/Ag-Bentonite and Chitosan/AgNPs-Bentonite beads at pH value of 7, (b) Photographed images of the corresponding composites beads in dried and swelling states.

*3.5 Antibacterial and antifungal activities*

Antibacterial and antifungal properties of pure Chitosan and raw Bentonite are presented in the Table 1. No activity was showed for these started sample. Chitosan/AgNPs-Bentonite against five different human pathogens strains Gram-negative (E. coli ATCC 25922, P. aeruginosa ATCC 27853), Gram-positive (S. aureus1 ATCC 25923, S. aureus2 ATCC 43300) bacteria and also as antifungal against Candida albicans ATCC10231 are displayed in **Fig. 6.** The inhibition zone for bacterial growth under and around the tested Chitosan/AgNPs-Bentonite beads was seen visually. The results of the antibacterial and antifungal activity tests suggest that the composites beads shown a great antibacterial activity against Gram-positive bacteria (S. aureus1 ATCC 25923 and S.aureus2 ATCC 43300) and Gram-negative bacteria (P. aeruginosa ATCC 27853), with a very clear inhibition zone with a diameter more than ~35 mm (**Fig. 7**). On the other hand,

the composite beads did not shown any antifungal activity. This antimicrobial activity of Chitosan/AgNPs-Bentonite is effectively related to the presence of loaded silver nanoparticles.

**Table 1**. Antibacterial activity of pure Chitosan and raw Bentonite

| Samples | S. aureus ATCC43300 | P. aeruginosa ATCC27853 | S. aureus ATCC25923 | E. coli ATCC25922 | Candida albicans ATCC10231 |
|---|---|---|---|---|---|
| Bentonite | 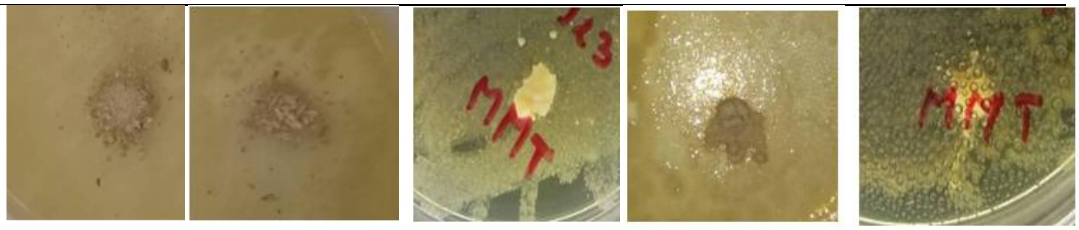 | | | | |
| Chitosan | 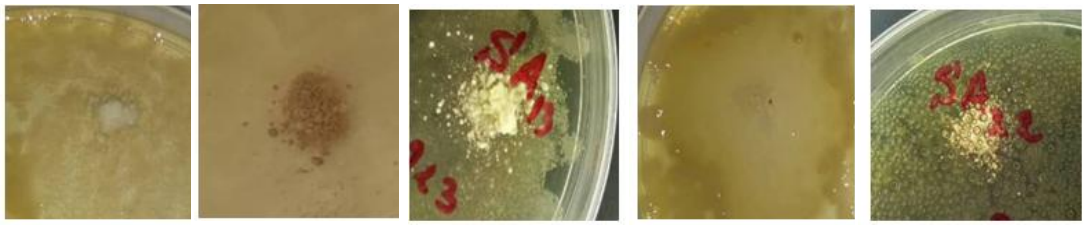 | | | | |

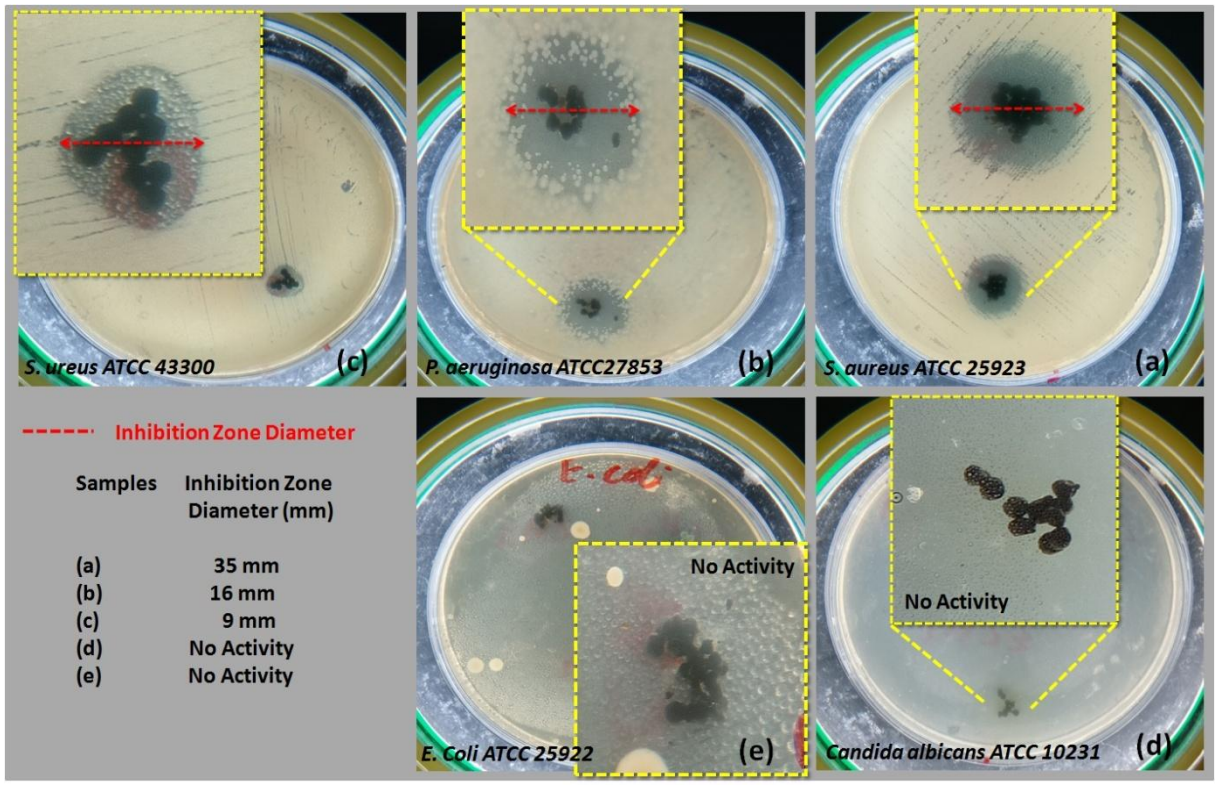


**Fig. 6** Antibacterial and antifungal activities of Chitosan/AgNPs-Bentonite material.

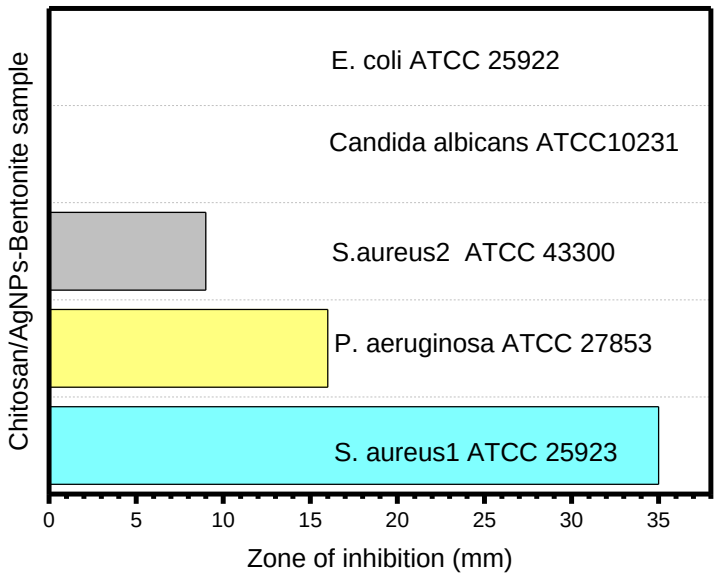


**Fig. 7** Diameter values of inhibition zones for Chitosan/AgNPs-Bentonite sample against pathogenic bacteria and fungal stains.

In the meantime, studies have been carried out to explore the application of silver nanoparticles and their antibacterial properties. Table 2 presents a summary of some works using different materials as supports for silver for antibacterial applications..

**Table 2**. Different antibacterial materials and their effects on bacteria

| Antibacterial Materials | Bacteria | Inhibition Zones (mm) | References |
|---|---|---|---|
| Cotton fibres loaded AgNPs | Escherichia coli | > 1.5 | [56] |
| Silver modified montmorillonites | Escherichia coli | 13.3 | [8] |
| Chitosan/AgNPs | Bacillus subtilis | 8.5 | [57] |
| | Escherichia coli | 8.7 | |
| AgNPs/onchitosans/montmorillonite | Bacillus subtilis | 8.0 | [57] |
| | Escherichia coli | 9.0 | |
| Ag/ montmorillonite | Escherichia coli | 14.5 | [58] |
| $Ag_2CO_3$/ montmorillonite | Escherichia coli | 8.4 | [58] |
| Silver/poly (lactic acid) | Staphylococcus aureus | 9.33 | [59] |
| nanocomposites | Escherichia coli | 10.33 | |
| Silver/montmorillonite/chitosan | Staphylococcus aureus | 8.8 | [60] |
| bionanocomposites | Escherichia coli | 8.7 | |
| AgNPs/zeolite | Shigella dysenteriae | 9.03 | [61] |
| | Staphylococcus aureus | 12.08 | |
| | Escherichia coli | 12.52 | |
| AgNPs intercalated kenyaite | Escherichia coli | 17 | [62] |
| Chlorhexidine loaded silver- | Staphylococcus aureus | > 40 | [63] |
| kaolinite | Enterococcus faecalis | 35 | |
| | Pseudomonas aeruginosa | >15 | |
| | Escherichia coli | >10 | |
| AgNPs-halloysite nanotube | Escherichia coli | 12 | [64] |
| nanocomposite | Staphylococcus aureus | 13 | |
| Chitosan/AgNPs-Bentonite | Staphylococcus aureus | 35 | This work |
| | P. aeruginosa | 16 | |

As shown in table 2, Chitosan/AgNPs-Bentonite composite displays a very high antibacterial activity and it is far more effective than other materials cited in the literature. Furthermore, it is also a broad-spectrum antibacterial material that will certainly find use in many areas

## 4. Conclusion

To sum up, Chitosan/AgNPs-Bentonite composite beads with a good antibacterial activity against Gram-positive and Gram-negative bacteria strains were successfully prepared. The X-ray diffraction, infrared FTIR spectroscopy and thermal TG analysis showed an establishment of strong interactions between the reactive groups of chitosan and bentonite interlayer materials, leading a partial intercalation of chitosan between the aluminosilicate sheets of bentonite. These strong interactions between chitosan and the mineral matrix result in a significant improvement in the thermal stability of the composites obtained, which increases with the bentonite content of the corresponding composite material. Compared to chitosan alone, the presence of bentonite in the composite materials prepared also leads to a marked improvement in their swelling property. In the case of chitosan/AgNPs-bentonite material, the XRD analysis shows the presence of AgNPs nanoparticles with an average diameter between 10nm and 25nm. The formation of these silver nanoparticles was confirmed also by UV-Vis DR spectroscopy. Evaluated as antibacterial and antifungal against pathogen strains, the Chitosan/AgNPs-Bentonite material displays a very high antibacterial activity against gram+ and gram-bacteria strains. However, no antifungal activity was observed for this sample. This biological activity is directly related to the presence of loaded silver nanoparticles.

*References*

**[1]** K. Kaviyarasu, N. Geetha, K. Kanimozhi, C.M. Magdalane, S. Sivaranjani, A. Ayeshamariam, J. Kennedy, M. Maaza, In vitro cytotoxicity effect and antibacterial performance of human lung epithelial cells A549 activity of zinc oxide doped TiO2 nanocrystals: investigation of bio-medical application by chemical method, Materials Science and Engineering: C 74 (2017) 325-333.

**[2]** K. Kaviyarasu, K. Kanimozhi, N. Matinise, C.M. Magdalane, G.T. Mola, J. Kennedy, M. Maaza, Antiproliferative effects on human lung cell lines A549 activity of cadmium selenide nanoparticles extracted from cytotoxic effects: investigation of bio-electronic application, Materials Science and Engineering: C 76 (2017) 1012-1025.

**[3]** A.M. Amanulla, S.J. Shahina, R. Sundaram, C.M. Magdalane, K. Kaviyarasu, D. Letsholathebe, S. Mohamed, J. Kennedy, M. Maaza, Antibacterial, magnetic, optical and humidity sensor studies of β-CoMoO4-Co3O4 nanocomposites and its synthesis and characterization, Journal of Photochemistry and Photobiology B: Biology 183 (2018) 233-241.

**[4]** C.M. Magdalane, K. Kaviyarasu, N. Matinise, N. Mayedwa, N. Mongwaketsi, D. Letsholathebe, G. Mola, N. AbdullahAl-Dhabi, M.V. Arasu, M. Henini, Evaluation on La2O3 garlanded ceria heterostructured binary metal oxide nanoplates for UV/visible light induced removal of organic dye from urban wastewater, South African journal of chemical engineering 26 (2018) 49-60.

**[5]** C.M. Magdalane, K. Kaviyarasu, A. Raja, M. Arularasu, G.T. Mola, A.B. Isaev, N.A. Al-Dhabi, M.V. Arasu, B. Jeyaraj, J. Kennedy, Photocatalytic decomposition effect of erbium doped cerium oxide nanostructures driven by visible light irradiation: Investigation of cytotoxicity, antibacterial growth inhibition using catalyst, Journal of Photochemistry and Photobiology B: Biology 185 (2018) 275-282.

**[6]** Z.A.M. Kebir, A. Mokhtar, M. Adjdir, A. Bengueddach, M. Sassi, Preparation and antibacterial activity of silver nanoparticles intercalated kenyaite materials, Materials Research Express (2018).

**[7]** A.R. Shahverdi, A. Fakhimi, H.R. Shahverdi, S. Minaian, Synthesis and effect of silver nanoparticles on the antibacterial activity of different antibiotics against Staphylococcus aureus and Escherichia coli, Nanomedicine: Nanotechnology, Biology and Medicine 3(2) (2007) 168-171.
**[8]** S. Magana, P. Quintana, D. Aguilar, J. Toledo, C. Angeles-Chavez, M. Cortes, L. Leon, Y. Freile-Pelegrín, T. Lopez, R.T. Sánchez, Antibacterial activity of montmorillonites modified with silver, Journal of Molecular Catalysis A: Chemical 281(1-2) (2008) 192-199.
**[9]** G. Franci, A. Falanga, S. Galdiero, L. Palomba, M. Rai, G. Morelli, M. Galdiero, Silver nanoparticles as potential antibacterial agents, Molecules 20(5) (2015) 8856-8874.
**[10]** H. Xu, X. Shi, H. Ma, Y. Lv, L. Zhang, Z. Mao, The preparation and antibacterial effects of dopa-cotton/AgNPs, Applied surface science 257(15) (2011) 6799-6803.
**[11]** G. Xu, X. Qiao, X. Qiu, J. Chen, Preparation and characterization of nano-silver loaded montmorillonite with strong antibacterial activity and slow release property, Journal of Materials Science & Technology 27(8) (2011) 685-690.
**[12]** H.-L. Su, C.-C. Chou, D.-J. Hung, S.-H. Lin, I.-C. Pao, J.-H. Lin, F.-L. Huang, R.-X. Dong, J.-J. Lin, The disruption of bacterial membrane integrity through ROS generation induced by nanohybrids of silver and clay, Biomaterials 30(30) (2009) 5979-5987.
**[13]** S.K. Pillai, S.S. Ray, M. Scriba, J. Bandyopadhyay, M. Roux-van der Merwe, J. Badenhorst, Microwave assisted green synthesis and characterization of silver/montmorillonite heterostructures with improved antimicrobial properties, Applied Clay Science 83 (2013) 315-321.
**[14]** E. Bennion, L. Sotheby's, Antique dental instruments, Sotheby's publications London1986.
**[15]** S. Raut, R. Ralegaonkar, S. Mandavgane, Development of sustainable construction material using industrial and agricultural solid waste: A review of waste-create bricks, Construction and building materials 25(10) (2011) 4037-4042.
**[16]** J. Sen, P. Prakash, N. De, Nano-clay composite and phyto-nanotechnology: a new horizon to food security issue in indian agriculture, Journal of Global Biosciences 4(5) (2015) 2187-2198.
**[17]** T. Tsoufis, L. Jankovic, D. Gournis, P.N. Trikalitis, T. Bakas, Evaluation of first-row transition metal oxides supported on clay minerals for catalytic growth of carbon nanostructures, Materials Science and Engineering: B 152(1-3) (2008) 44-49.
**[18]** R.S. Varma, Clay and clay-supported reagents in organic synthesis, Tetrahedron 58(7) (2002) 1235-1255.
**[19]** M. Chiban, M. Zerbet, G. Carja, F. Sinan, Application of low-cost adsorbents for arsenic removal: A review, Journal of Environmental Chemistry and Ecotoxicology 4(5) (2012) 91-102.
**[20]** L.-n. Shi, X. Zhang, Z.-l. Chen, Removal of chromium (VI) from wastewater using bentonite-supported nanoscale zero-valent iron, Water research 45(2) (2011) 886-892.
**[21]** S.C. Motshekga, S.S. Ray, M.S. Onyango, M.N. Momba, Microwave-assisted synthesis, characterization and antibacterial activity of Ag/ZnO nanoparticles supported bentonite clay, Journal of hazardous materials 262 (2013) 439-446.
**[22]** D. Bouazza, H. Miloudi, M. Adjdir, A. Tayeb, A. Boos, Competitive adsorption of Cu (II) and Zn (II) on impregnate raw Algerian bentonite and efficiency of extraction, Applied Clay Science 151 (2018) 118-123.
**[23]** Y.S. Reddy, C.M. Magdalane, K. Kaviyarasu, G.T. Mola, J. Kennedy, M. Maaza, Equilibrium and kinetic studies of the adsorption of acid blue 9 and Safranin O from aqueous solutions by MgO decked FLG coated Fuller's earth, Journal of Physics and Chemistry of Solids 123 (2018) 43-51.
**[24]** F. Bergaya, G. Lagaly, General introduction: clays, clay minerals, and clay science, Developments in clay science, Elsevier2013, pp. 1-19.
**[25]** V.N. Tirtom, A. Dinçer, S. Becerik, T. Aydemir, A. Çelik, Comparative adsorption of Ni (II) and Cd (II) ions on epichlorohydrin crosslinked chitosan–clay composite beads in aqueous solution, Chemical Engineering Journal 197 (2012) 379-386.
**[26]** A. Bée, L. Obeid, R. Mbolantenaina, M. Welschbillig, D. Talbot, Magnetic chitosan/clay beads: A magsorbent for the removal of cationic dye from water, Journal of Magnetism and Magnetic Materials 421 (2017) 59-64.
**[27]** A. Mokhtar, A. Djelad, A. Bengueddach, M. Sassi, CuNPs-magadiite/chitosan nanocomposite beads as advanced antibacterial agent: Synthetic path and characterization, International journal of biological macromolecules 118 (2018) 2149-2155.
**[28]** Y.-S. Han, S.-H. Lee, K.H. Choi, I. Park, Preparation and characterization of chitosan–clay nanocomposites with antimicrobial activity, Journal of Physics and Chemistry of Solids 71(4) (2010) 464-467.
**[29]** K. Kurita, Chitin and chitosan: functional biopolymers from marine crustaceans, Marine Biotechnology 8(3) (2006) 203.

**[30]** Y. Liu, Z. Zhong, Extraction of heavy metals, dichromate anions and rare metals by new calixarene-chitosan polymers, Journal of Inorganic and Organometallic Polymers and Materials 28(3) (2018) 962-967.
**[31]** M. Rinaudo, Chitin and chitosan: properties and applications, Progress in polymer science 31(7) (2006) 603-632.
**[32]** C. Branca, G. D'Angelo, C. Crupi, K. Khouzami, S. Rifici, G. Ruello, U. Wanderlingh, Role of the OH and NH vibrational groups in polysaccharide-nanocomposite interactions: A FTIR-ATR study on chitosan and chitosan/clay films, Polymer 99 (2016) 614-622.
**[33]** Z. Cherifi, B. Boukoussa, A. Zaoui, M. Belbachir, R. Meghabar, Structural, morphological and thermal properties of nanocomposites poly (GMA)/clay prepared by ultrasound and in-situ polymerization, Ultrasonics Sonochemistry (2018).
**[34]** B. Liu, J. Luo, X. Wang, J. Lu, H. Deng, R. Sun, Alginate/quaternized carboxymethyl chitosan/clay nanocomposite microspheres: preparation and drug-controlled release behavior, Journal of Biomaterials Science, Polymer Edition 24(5) (2013) 589-605.
**[35]** S. Farhoudian, M. Yadollahi, H. Namazi, Facile synthesis of antibacterial chitosan/CuO bio-nanocomposite hydrogel beads, International journal of biological macromolecules 82 (2016) 837-843.
**[36]** M. Zahraoui, A. Mokhtar, M. Adjdir, F. Bennabi, R. Khaled, A. Djelad, A. Bengueddach, M. Sassi, Preparation of Al-magadiite material, copper ions exchange and effect of counter-ions: antibacterial and antifungal applications, Research on Chemical Intermediates (2018) 1-12.
**[37]** A. Saravanakumar, M. Ganesh, J. Jayaprakash, H.T. Jang, Biosynthesis of silver nanoparticles using Cassia tora leaf extract and its antioxidant and antibacterial activities, Journal of Industrial and Engineering Chemistry 28 (2015) 277-281.
**[38]** J. Balavijayalakshmi, V. Ramalakshmi, Carica papaya peel mediated synthesis of silver nanoparticles and its antibacterial activity against human pathogens, Journal of Applied Research and Technology 15(5) (2017) 413-422.
**[39]** T. Kayalvizhi, S. Ravikumar, P. Venkatachalam, Green synthesis of metallic silver nanoparticles using Curculigo orchioides rhizome extracts and evaluation of its antibacterial, larvicidal, and anticancer activity, Journal of Environmental Engineering 142(9) (2016) C4016002.
**[40]** C. Paluszkiewicz, M. Holtzer, A. Bobrowski, FTIR analysis of bentonite in moulding sands, Journal of Molecular Structure 880(1-3) (2008) 109-114.
**[41]** F.G. Alabarse, R.V. Conceição, N.M. Balzaretti, F. Schenato, A.M. Xavier, In-situ FTIR analyses of bentonite under high-pressure, Applied Clay Science 51(1-2) (2011) 202-208.
**[42]** H. Moussout, H. Ahlafi, M. Aazza, O. Zegaoui, C. El Akili, Adsorption studies of Cu (II) onto biopolymer chitosan and its nanocomposite 5% bentonite/chitosan, Water Science and Technology 73(9) (2016) 2199-2210.
**[43]** A. Mokhtar, A. Djelad, A. Bengueddach, M. Sassi, Biopolymer-layered polysilicate micro/nanocomposite based on chitosan intercalated in magadiite, Research on Chemical Intermediates 1-10.
**[44]** F.G. Torres, J. Arroyo, R. Alvarez, S. Rodriguez, O. Troncoso, D. López, Molecular dynamics of carboxymethyl κ/ι-hybrid carrageenan films doped with NH4I, Polymer-Plastics Technology and Engineering (2018) 1-14.
**[45]** A.R. Nesic, S.J. Velickovic, D.G. Antonovic, Characterization of chitosan/montmorillonite membranes as adsorbents for Bezactiv Orange V-3R dye, Journal of hazardous materials 209 (2012) 256-263.
**[46]** A. Mokhtar, A. Djelad, A. Bengueddach, M. Sassi, Structural and Antibacterial Properties of H y Zn x Na 2− x Si 14 O 29 nH 2 O Layered Silicate Compounds, Prepared by Ion-Exchange Reaction, Journal of Inorganic and Organometallic Polymers and Materials 1-10.
**[47]** J.P. Montañez, S. Gómez, A.N. Santiago, L.B. Pierella, TiO2 Supported on HZSM-11 Zeolite as Efficient Catalyst for the Photodegradation of Chlorobenzoic Acids, Journal of the Brazilian Chemical Society 26(6) (2015) 1191-1200.
**[48]** S.A. Babu, H.G. Prabu, Synthesis of AgNPs using the extract of Calotropis procera flower at room temperature, Materials Letters 65(11) (2011) 1675-1677.
**[49]** M. Zahran, H.B. Ahmed, M. El-Rafie, Alginate mediate for synthesis controllable sized AgNPs, Carbohydrate polymers 111 (2014) 10-17.
**[50]** H. Moussout, H. Ahlafi, M. Aazza, A. Amechrouq, Bentonite/chitosan nanocomposite: Preparation, characterization and kinetic study of its thermal degradation, Thermochimica Acta 659 (2018) 191-202.
**[51]** A. Mokhtar, Z.A.K. Medjhouda, A. Djelad, A. Boudia, A. Bengueddach, M. Sassi, Structure and intercalation behavior of copper II on the layered sodium silicate magadiite material, Chemical Papers 72(1) (2018) 39-50.

**[52]** X. Wang, Y. Du, J. Yang, X. Wang, X. Shi, Y. Hu, Preparation, characterization and antimicrobial activity of chitosan/layered silicate nanocomposites, Polymer 47(19) (2006) 6738-6744.
**[53]** K. Gupta, M.R. Kumar, Drug release behavior of beads and microgranules of chitosan, Biomaterials 21(11) (2000) 1115-1119.
**[54]** G. Pasparakis, N. Bouropoulos, Swelling studies and in vitro release of verapamil from calcium alginate and calcium alginate–chitosan beads, International journal of pharmaceutics 323(1-2) (2006) 34-42.
**[55]** Q. Wang, X. Xie, X. Zhang, J. Zhang, A. Wang, Preparation and swelling properties of pH-sensitive composite hydrogel beads based on chitosan-g-poly (acrylic acid)/vermiculite and sodium alginate for diclofenac controlled release, International journal of biological macromolecules 46(3) (2010) 356-362.
**[56]** S. Ravindra, Y.M. Mohan, N.N. Reddy, K.M. Raju, Fabrication of antibacterial cotton fibres loaded with silver nanoparticles via "Green Approach", Colloids and Surfaces A: Physicochemical and Engineering Aspects 367(1-3) (2010) 31-40.
**[57]** J.S. Gabriel, V.A. Gonzaga, A.L. Poli, C.C. Schmitt, Photochemical synthesis of silver nanoparticles on chitosans/montmorillonite nanocomposite films and antibacterial activity, Carbohydrate polymers 171 (2017) 202-210.
**[58]** L.F. Giraldo, P. Camilo, T. Kyu, Incorporation of silver in montmorillonite-type phyllosilicates as potential antibacterial material, Current opinion in chemical engineering 11 (2016) 7-13.
**[59]** K. Shameli, M.B. Ahmad, W.M.Z.W. Yunus, N.A. Ibrahim, R.A. Rahman, M. Jokar, M. Darroudi, Silver/poly (lactic acid) nanocomposites: preparation, characterization, and antibacterial activity, International journal of nanomedicine 5 (2010) 573.
**[60]** K. Shameli, M.B. Ahmad, W.M.Z.W. Yunus, A. Rustaiyan, N.A. Ibrahim, M. Zargar, Y. Abdollahi, Green synthesis of silver/montmorillonite/chitosan bionanocomposites using the UV irradiation method and evaluation of antibacterial activity, International journal of nanomedicine 5 (2010) 875.
**[61]** K. Shameli, M.B. Ahmad, M. Zargar, W.M.Z.W. Yunus, N.A. Ibrahim, Fabrication of silver nanoparticles doped in the zeolite framework and antibacterial activity, International journal of nanomedicine 6 (2011) 331.
**[62]** Z.A.M. Kebir, M. Adel, M. Adjdir, A. Bengueddach, M. Sassi, Preparation and antibacterial activity of silver nanoparticles intercalated kenyaite materials, Materials Research Express 5(8) (2018) 085021.
**[63]** S.K. Jou, N.A.N.N. Malek, Characterization and antibacterial activity of chlorhexidine loaded silver-kaolinite, Applied Clay Science 127 (2016) 1-9.
**[64]** Y. Zhang, Y. Chen, H. Zhang, B. Zhang, J. Liu, Potent antibacterial activity of a novel silver nanoparticle-halloysite nanotube nanocomposite powder, Journal of inorganic biochemistry 118 (2013) 59-64.